

# Discrete-dipole approximation with polarizabilities that account for both finite wavelength and target geometry

Matthew J. Collinge and B. T. Draine

Princeton University Observatory, Princeton, New Jersey 08544-1001

Received November 12, 2003; revised manuscript received March 24, 2004; accepted May 5, 2004

The discrete-dipole approximation (DDA) is a powerful method for calculating absorption and scattering by targets that have sizes smaller than or comparable with the wavelength of the incident radiation. We present a new prescription—the surface-corrected-lattice-dispersion relation (SCLDR)—for assigning the dipole polarizabilities while taking into account both target geometry and finite wavelength. We test the SCLDR in DDA calculations for spherical and ellipsoidal targets and show that for a fixed number of dipoles, the SCLDR prescription results in increased accuracy in the calculated cross sections for absorption and scattering. We discuss extension of the SCLDR prescription to irregular targets. © 2004 Optical Society of America  
*OCIS codes:* 000.4430, 240.0240, 260.2110, 290.5850.

## 1. INTRODUCTION

The discrete-dipole approximation (DDA) is a numerical technique for calculating scattering and absorption of electromagnetic radiation by targets with sizes smaller than or comparable with the incident wavelength. The method consists of approximating the target by an array of polarizable points (dipoles), assigning polarizabilities at these locations based on the physical properties of the target, and solving self-consistently for the polarization at each location in the presence of an incident radiation field. This procedure can yield arbitrarily accurate results as the number of dipoles used to approximate the target is increased, with the caveat that the number of dipoles required to reach a given level of accuracy can depend strongly on the refractive index of the target. In reality, computational considerations limit the number of dipoles that can be used. Hence methods for increasing the accuracy for a fixed number of dipoles are desirable.

A key factor in determining the level of accuracy that can be reached for a given number of dipoles is the prescription for assigning dipole polarizabilities. In this work, we present a new polarizability prescription that takes into account both target geometry and the finite wavelength of incident radiation. We test this technique in calculations of absorption and scattering by spherical and ellipsoidal targets and show that for a fixed number of dipoles, it generally provides increased accuracy over previous methods. In Section 2 we discuss previous polarizability prescriptions and develop the new method. In Section 3 we present calculations testing the new prescription, and in Section 4 we discuss our results.

## 2. POLARIZABILITY PRESCRIPTIONS

A fundamental requirement of the DDA is that the inter-dipole separation  $d$  be small compared with the wavelength of incident radiation,  $kd \ll 1$ , where  $k \equiv \omega/c$  is the

wave number *in vacuo*. Here we will assume the dipoles to be located on a cubic lattice with lattice constant  $d$ , as this facilitates use of fast-Fourier-transform techniques.<sup>1</sup>

In the first implementations of the DDA<sup>2</sup> the so-called Clausius–Mossotti relation (CMR) was used to determine the dipole polarizabilities. In this procedure, the polarizability  $\alpha$  is given as a function of the (complex) refractive index  $m$  in the form

$$\alpha_{\text{CMR}} = \frac{3d^3}{4\pi} \left( \frac{m^2 - 1}{m^2 + 2} \right). \quad (1)$$

This approach is valid in the infinite wavelength limit of the DDA,  $kd \rightarrow 0$ .

Draine<sup>3</sup> showed that for finite wavelengths, the optical theorem requires that the polarizabilities include a radiative-reaction correction of the form

$$\alpha = \frac{\alpha^{(\text{nr})}}{1 - (2/3)i(\alpha^{(\text{nr})}/d^3)(kd)^3}, \quad (2)$$

where  $\alpha^{(\text{nr})}$  is the nonradiative polarizability, that is, before any radiative-reaction correction is applied. Draine<sup>3</sup> used  $\alpha_{\text{CMR}}$  as the nonradiative polarizability.

Based on analysis of an integral formulation of the scattering problem, Goedecke and O'Brien<sup>4</sup> and Hage and Greenberg<sup>5</sup> suggested further corrections to the CMR polarizability of order  $(kd)^2$ . Draine and Goodman<sup>6</sup> studied electromagnetic wave propagation on an infinite lattice; they required that the lattice reproduce the dispersion relation of a continuum medium. In this lattice-dispersion-relation (LDR) approach, the radiative-reaction correction emerges naturally, and the polarizability is given [to order  $(kd)^3$ ] by

$$\alpha_{\text{LDR}} = \frac{\alpha^{(0)}}{1 + (\alpha^{(0)}/d^3)[(b_1 + m^2 b_2 + m^2 b_3 S)(kd)^2 - (2/3)i(kd)^3]}, \quad (3)$$

where  $\alpha^{(0)} = \alpha_{\text{CMR}}$  is the polarizability in the limit  $kd \rightarrow 0$ ,  $b_1 = -1.8915316$ ,  $b_2 = 0.1648469$ ,  $b_3 = -1.7700004$ , and  $S$  is a function of the propagation direction and polarization of the incident wave.  $S$  is given as

$$S = \sum_j (\mathbf{a}_j \mathbf{e}_j)^2, \quad (4)$$

where  $\mathbf{a}$  and  $\mathbf{e}$  are the unit propagation and polarization vectors, and the directions  $j = 1, 2, 3$  correspond to the axes of the dipole lattice. Note that Eq. (4) gives  $S = 0$  for waves propagating along any of the lattice axes. This method includes corrections to  $\mathcal{O}[(kd)^3]$  for the finite wavelength of incident radiation, and by construction it accurately reproduces wave propagation in an infinite medium. Its primary limitation is that the accuracy in computing absorption cross sections of finite targets (for a given number of dipoles) degrades rapidly as the imaginary part of the refractive index  $m$  becomes large [e.g., for  $\text{Im}(m) \geq 2$ ].

Recently Rahmani, Chaumet, and Bryant<sup>7</sup> (RCB) proposed a new method for assigning the polarizabilities that takes into account the effects of target geometry on the local electric field at each dipole site. Consider a continuum target in a static, uniform applied field  $\mathbf{E}^0$ . At each location  $j$  in the target, the macroscopic electric field  $\mathbf{E}_j^{\text{mac}}$  is linearly related to  $\mathbf{E}^0$ :

$$\mathbf{E}_j^{\text{mac}} = \mathbf{C}_j^{-1} \mathbf{E}^0, \quad (5)$$

where  $\mathbf{C}_j^{-1}$  is a  $3 \times 3$  tensor that will in general depend on location  $j$ , the global geometry of the target, and its (possibly nonuniform) composition. If we now represent the target by a dipole array and require that the electric dipole moment  $\mathbf{P}_j$  of dipole  $j$  be equal to  $d^3$  times the macroscopic polarization density at location  $j$ , we obtain

$$\mathbf{P}_j = d^3 \left( \frac{m_j^2 - 1}{4\pi} \right) \mathbf{E}_j^{\text{mac}} = d^3 \left( \frac{m_j^2 - 1}{4\pi} \right) \mathbf{C}_j^{-1} \mathbf{E}^0, \quad (6)$$

where  $m_j$  is the refractive index at location  $j$ . If  $\alpha_j$  is the polarizability tensor of dipole  $j$ , then

$$\mathbf{P}_j = \alpha_j \left[ \mathbf{E}^0 - \sum_{k \neq j} \mathbf{A}_{jk} \mathbf{P}_k \right], \quad (7)$$

where  $-\mathbf{A}_{jk} \mathbf{P}_k$  is the contribution to the electric field at location  $j$  due to dipole  $\mathbf{P}_k$  at location  $k$  (this defines the  $3 \times 3$  tensors  $\mathbf{A}_{jk}$ ). Equation (7) is quite general; restricting ourselves again to the static case, we can substitute Eq. (6) into Eq. (7) to obtain

$$\alpha_{\text{RCB},j} = d^3 \left( \frac{m_j^2 - 1}{4\pi} \right) \Lambda_j^{-1}, \quad (8)$$

where the  $3 \times 3$  tensors

$$\Lambda_j \equiv \mathbf{C}_j - \sum_{k \neq j} \mathbf{A}_{jk} \left( \frac{m_k^2 - 1}{4\pi} \right) d^3 \mathbf{C}_k^{-1} \mathbf{C}_j \quad (9)$$

can be evaluated (and easily inverted) if the  $\mathbf{C}_j$  are known. By construction, the RCB polarizability is exact in the static limit. The operation  $\sum_{k \neq j} \mathbf{A}_{jk} (m_k^2 - 1) \mathbf{C}_k^{-1}$  in Eq. (9) can be represented as a convolution and efficiently evaluated by using fast-Fourier-transform techniques.<sup>1</sup> In practice, the computational effort needed for this step contributes negligibly to the overall computing time in DDA calculations.

The RCB approach requires that the tensors  $\mathbf{C}_j$  first be obtained. In general, this will require solving the electrostatic problem numerically to a high level of accuracy, which is not the focus of this paper. For targets composed of homogeneous, isotropic materials and with certain simple geometries,  $\mathbf{C}_j$  can be obtained analytically and does not depend on location within the target. This holds for ellipsoids, infinite slabs, and infinite cylinders. In these special cases  $\mathbf{C}_j$  can be expressed in the form

$$\mathbf{C}_j = 1 + \left( \frac{m^2 - 1}{4\pi} \right) \mathbf{L}, \quad (10)$$

where  $\mathbf{L}$  is a  $3 \times 3$  “depolarization tensor.” For an ellipsoid  $\mathbf{L}$  is diagonal in a frame in which the axes are chosen to be the principal axes of the ellipsoid. The depolarization factors are obtained by numerical quadrature (see §5.3 of Bohren and Huffman<sup>8</sup>); the diagonal elements of  $\mathbf{L}$  for an ellipsoid with 1:2:3 axial ratios are  $L_{11} = 0.5765453$ ,  $L_{22} = 0.2671541$ , and  $L_{33} = 0.1563007$  (where the largest eigenvalue corresponds to the shortest axis) to a precision of  $5 \times 10^{-7}$ . For a sphere, the diagonal elements of  $\mathbf{L}$  all have the degenerate value  $L = 1/3$  (i.e.,  $L$  is a scalar with this value).

In the present work, we combine the LDR and RCB approaches to obtain a polarizability prescription that accounts both for finite wavelength and for local field corrections arising from target geometry. We adopt  $\alpha_{\text{RCB},j}$  as the polarizability  $\alpha_j^{(0)}$  of dipole  $j$  in the limit  $kd \rightarrow 0$  and apply corrections up to  $\mathcal{O}[(kd)^3]$  based on the LDR. A further analysis of the electromagnetic dispersion relation of a rectangular lattice<sup>9</sup> called into question the factor  $S$  as given in Eq. (4) and used by Draine and Goodman,<sup>6</sup> finding that it should instead be  $S_j = \alpha_j^2$ , where  $j = 1, 2, 3$  are the axes of the dipole lattice. In general  $\alpha_{\text{RCB},j}$  is not diagonal in the lattice frame; to apply corrections analogous to the LDR, we define a correction matrix  $\mathbf{B}$  (see below). The surface-corrected-lattice-dispersion-relation (SCLDR) polarizability is given by

$$\alpha_{\text{SCLDR},j} = \alpha_{\text{RCB},j} [1 + (\alpha_{\text{RCB},j}/d^3) \mathbf{B}]^{-1}, \quad (11)$$

where

$$B_{ij} = (b_1 + m^2 b_2 + m^2 b_3 a_i^2 \delta_{ij})(kd)^2 - (2/3)i(kd)^3, \quad (12)$$

in which  $\delta_{ij}$  is the usual Kronecker delta. In Section 3 we test this new prescription in calculations of absorption and scattering by spherical and ellipsoidal targets.

### 3. SPHERE AND ELLIPSOID CALCULATIONS

For a continuum target of volume  $V$  we define the effective radius  $a_{\text{eff}} \equiv (3V/4\pi)^{1/3}$ , the radius of a sphere of equal volume. The target is approximated by an array of  $N$  dipoles located on a cubic lattice with the dipole locations selected by some criterion designed to approximate the shape of the original target. The interdipole spacing is then set to  $d = (V/N)^{1/3}$ .

For a given orientation of the dipole array relative to the incident wave, we calculate the cross sections  $C_{\text{sca}}$  and  $C_{\text{abs}}$  for scattering and absorption and the dimensionless efficiency factors  $Q_{\text{sca}} \equiv C_{\text{sca}}/\pi a_{\text{eff}}^2$ ,  $Q_{\text{abs}} \equiv C_{\text{abs}}/\pi a_{\text{eff}}^2$ .

To test the performance of the SCLDR polarizability prescription against previous results, we performed a series of calculations with the DDA code DDSCAT<sup>10</sup> modified to permit use of the SCLDR polarizabilities. We computed  $Q_{\text{sca}}$  and  $Q_{\text{abs}}$  for spherical targets with a range of refractive indices and for a range of scattering parameters  $x = 2\pi a_{\text{eff}}/\lambda = ka_{\text{eff}}$ , using three different approaches for assigning the dipole polarizabilities: LDR, RCB, and SCLDR. Spherical targets were employed because the exact optical properties can be readily calculated by use of Mie theory. We also performed a similar but more limited set of calculations for ellipsoidal targets.

We tested the LDR, RCB, and SCLDR prescriptions for a number of different refractive indices in the region of the complex plane with  $\text{Re}(m) \leq 5$  and  $\text{Im}(m) \leq 4$ . Figures 1 and 2 show the results of calculations for spheres with refractive indices  $m = 1.33 + 0.01i$  and  $m = 5 + 4i$  and with each approximated by an array of  $N = 7664$  dipoles. Because the dipole array is not rotationally symmetric,  $Q_{\text{sca}}$  and  $Q_{\text{abs}}$  calculated with the DDA depend in general on the target orientation; we perform calculations for 12 orientations, and we show the average and range of the results. We calculate the fractional errors in  $Q_{\text{sca}}$  and  $Q_{\text{abs}}$  by comparison with exact results obtained with Mie theory:

$$\text{Frac.Err.} \equiv \frac{Q(\text{DDA}) - Q(\text{Mie})}{Q(\text{Mie})}. \quad (13)$$

In previous work<sup>11</sup> it was recommended that the DDA be used only when  $|m|kd \leq 1$ , or—a more stringent condition— $|m|kd < 0.5$  if the DDA is to be used to calculate the differential scattering cross section. In the present work we find that when the SCLDR polarizabilities are used, the fractional errors in  $Q_{\text{sca}}$  and  $Q_{\text{abs}}$  are relatively insensitive to  $x$  provided  $|m|kd \leq 0.8$ , which we adopt as an operational validity criterion. Figures 1 and 2 show results for values of  $x$  satisfying  $|m|kd \leq 0.8$ .

From Fig. 1 it is clear that the LDR and SCLDR prescriptions provide approximately equal levels of accuracy in the  $|m - 1| \leq 1/2$  regime, while the RCB prescription does not perform as well. Figure 2 shows that at the other extreme of  $\text{Re}(m) \gg 1$  and  $\text{Im}(m) \gg 1$ , the LDR approach results in large errors, especially in the calculated absorption cross sections, while the RCB and SCLDR prescriptions perform approximately equally well.

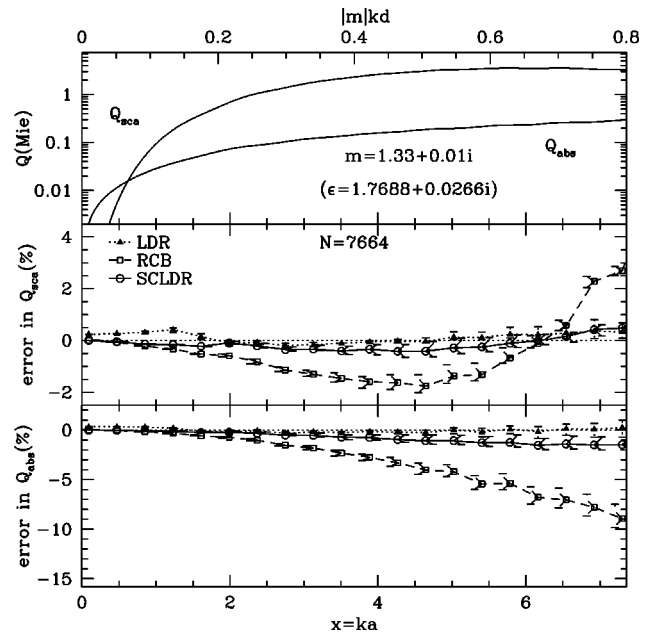


Fig. 1. Comparison of scattering and absorption efficiency factors  $Q_{\text{sca}}$  and  $Q_{\text{abs}}$  computed for a pseudosphere of  $N = 7664$  dipoles and refractive index  $m = 1.33 + 0.01i$ , averaged over 12 orientations, and using three different polarizability prescriptions: LDR, RCB, and SCLDR. The horizontal axis shows (top)  $|m|kd$  (the phase shift in radians within one lattice spacing) and (bottom) the scattering parameter  $x = ka$ . Error bars indicate the ranges of  $Q$  values obtained for the individual orientations. The top panel shows the results of Mie theory calculations; the lower panels show the fractional error in  $Q_{\text{sca}}$  and  $Q_{\text{abs}}$ . The SCLDR and LDR prescriptions are clearly preferred over the RCB prescription for this case.

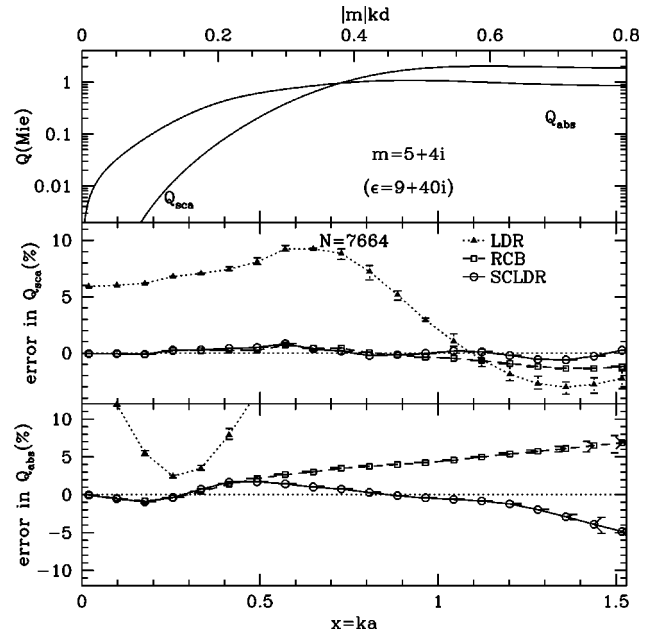


Fig. 2. Same as Fig. 1, but for refractive index  $m = 5 + 4i$ . The SCLDR and RCB prescriptions are clearly preferred over the LDR for this case, with the SCLDR being somewhat superior to the RCB prescription.

In Figs. 3 and 4 we show the convergence behavior of the different polarizability prescriptions as the number of dipoles  $N$  is increased for spherical targets with selected refractive indices; the refractive indices have been chosen

to sample the region of the complex plane discussed in the previous paragraphs. Again the fractional error in  $Q_{\text{abs}}$  and  $Q_{\text{sca}}$  are calculated with respect to the exact values from Mie theory; in all cases, as  $N$  is increased the DDA results converge toward the exact results. The SCLDR method performs comparably with or better than the RCB and LDR prescriptions throughout this region of the complex-refractive-index plane. This illustrates an advantage of the SCLDR approach over these previous techniques: It performs well over a large range of real and imaginary components of the refractive index.

Figures 5 and 6 extend the results shown in Figs. 3 and 4 to targets of a more general shape: ellipsoids with 1:2:3 axial ratios. As  $N$  is increased, the approximation inherent in the DDA (i.e., that a continuum target can be represented by a dipole array with finite lattice spacing) becomes better and better, and the DDA results converge toward exact results; this expectation is confirmed by the results shown for spheres in Figs. 3 and 4. For the ellipsoidal targets, we have estimated the asymptotic values of  $Q_{\text{sca}}$  and  $Q_{\text{abs}}$  by assuming these to be linear functions of  $N^{-1/3}$ , extrapolating to  $N^{-1/3} \rightarrow 0$  for each polarizability prescription, and taking the average of the results from the different prescriptions. The close similarity of

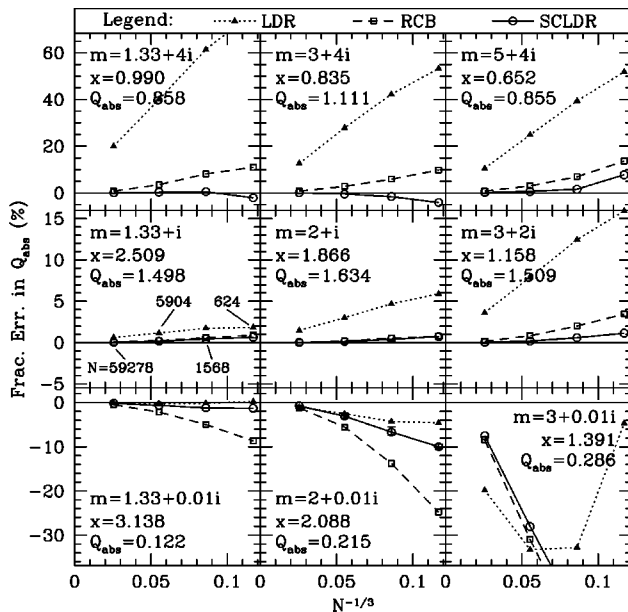


Fig. 3. Fractional error in  $Q_{\text{abs}}$  averaged over 12 orientations for spheres with different refractive indices as a function of  $N^{-1/3}$ , where  $N$  is the number of dipoles in the range 624–59,278. Calculations are shown for the LDR, RCB, and SCLDR polarizability prescriptions; the symbolic scheme is the same as in Fig. 1. Error bars in the lower middle panel indicate the typical ranges of  $Q$  values obtained for the individual orientations, as in Fig. 1 (shown for SCLDR prescription only). Refractive indices  $m$ , scattering parameters  $x = ka$ , and exact values of  $Q_{\text{abs}}$  computed from Mie theory are shown inside each panel. The scattering parameters are chosen so that  $|m|kd \approx 0.8$  (the approximate limit of applicability of the DDA) for the smallest number ( $N = 624$ ) of dipoles. The convergence with increasing  $N$  is quite smooth in all regions of the complex  $m$  plane with the exception of  $m = 3 + 0.01i$ . In almost every case shown, fractional errors  $<2\%$  (and often significantly lower) can be achieved for  $N \approx 6000$  dipoles. We find that for calculating  $Q_{\text{abs}}$ , the SCLDR is comparable with or superior in accuracy to the LDR and RCB prescriptions throughout the region of  $m$  space shown.

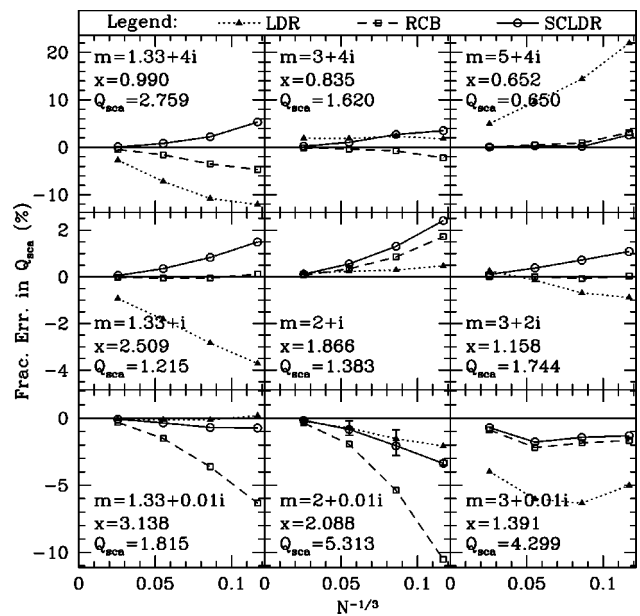


Fig. 4. Same as Fig. 3, except that fractional errors in  $Q_{\text{sca}}$  are plotted. Again, the SCLDR prescription is comparable with or superior to the LDR and RCB prescriptions for most  $m$  values. The SCLDR prescription produces fractional errors  $<2\%$  in all cases for  $N \approx 6000$  dipoles. In some cases, all three prescriptions produce fractional errors  $<2\%$  even for small  $N$ .

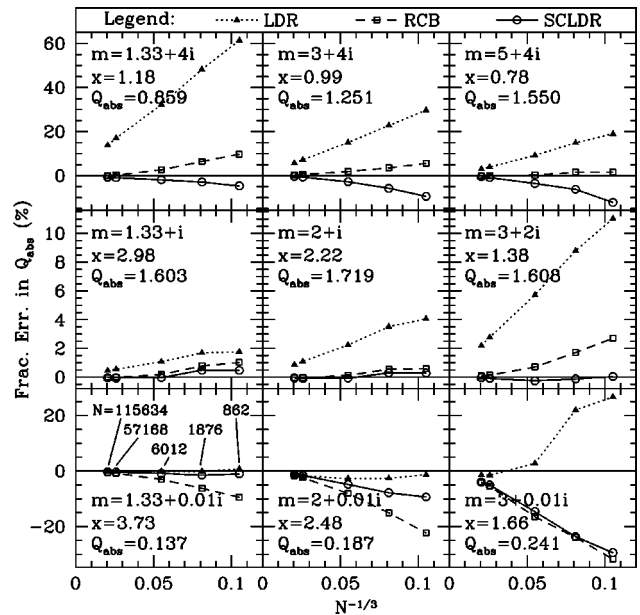


Fig. 5. Same as Fig. 3, but for ellipsoids with approximately 1:2:3 axial ratios. Fractional errors have been estimated based on comparison with an extrapolation of the convergence behavior of the three polarizability prescriptions as described in Section 3. Again the SCLDR prescription is comparable with or superior to the LDR and RCB prescriptions for calculating  $Q_{\text{abs}}$  throughout the region of the complex  $m$  plane sampled.

the results of these calculations to those shown in Figs. 3 and 4 demonstrates that the SCLDR prescription provides the same benefits in calculations for ellipsoidal targets as for spheres. We note that for ellipsoids with values of  $m$  with large imaginary parts [typically  $\text{Im}(m) > 1$ ], the RCB prescription can provide somewhat higher accuracy, particularly in calculations of  $Q_{\text{sca}}$ .

For an isotropic material with refractive index  $m$ , the Clausius–Mossotti polarizability  $\alpha_{\text{CMR}}$  has triply degenerate eigenvalues  $\alpha_{\text{CMR}} = (m^2 - 1)d^3/4\pi$ . We have calculated the eigenvalues  $\alpha$  of  $\alpha_{\text{SCLDR},j}$  for  $|m|kd \rightarrow 0$  (in which case  $\alpha_{\text{SCLDR},j} \rightarrow \alpha_{\text{RCB},j}$ ) at each occupied lattice

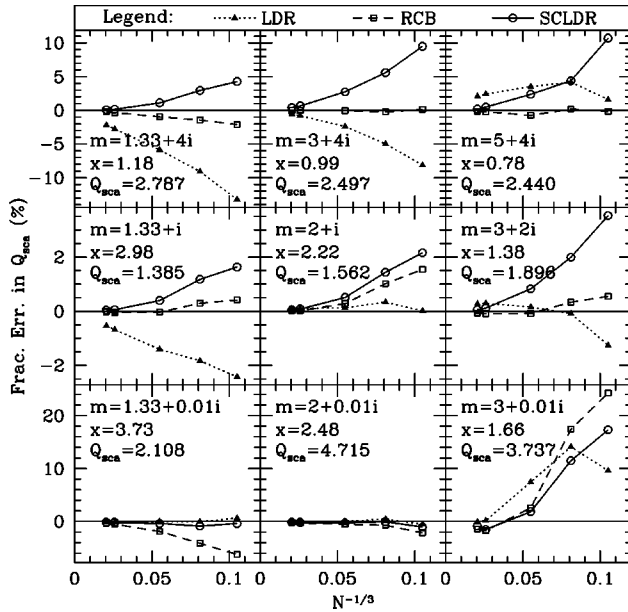


Fig. 6. Same as Fig. 5, except that fractional errors in  $Q_{\text{sca}}$  are plotted. The SCLDR prescription is comparable with or superior to LDR for all values of  $m$  and to RCB for values of  $m$  with small imaginary parts, while RCB is superior to SCLDR for values of  $m$  with large imaginary parts. In most cases, the SCLDR prescription produces fractional errors  $< 2\%$  for  $N \approx 6000$  dipoles.

site  $j$  in a 1:2:3 ellipsoid with  $m = 5 + 4i$ . Figure 7 (left panel) shows the distribution of the fractional difference of the eigenvalues  $\alpha$  from  $\alpha_{\text{CMR}}$ . The left panel shows that the deviations are appreciable (fractional difference exceeding  $\sim 20\%$ ) for 47% of the lattice sites when  $N = 90$ , but for only 9% of the lattice sites when  $N = 43,416$ . In this example the fraction of the eigenvalues deviating by  $> 20\%$  is  $\approx 0.30(N/1000)^{-1/3}$  for  $N \geq 500$ , approximately equal to the fraction of the dipoles located within a surface layer of thickness  $\sim 0.6d$ . The right panel of Fig. 7 shows the eigenvalue deviations as a function of distance from the surface of the ellipsoid: the eigenvalues deviating from  $\alpha_{\text{CMR}}$  by more than  $\sim 20\%$  are, as expected, associated exclusively with dipoles located within a distance  $\sim d$  of the surface.

#### 4. CONCLUSION

We introduce a new DDA polarizability prescription—the surface-corrected-lattice-dispersion relation (SCLDR). This technique builds on the previous work of Rahmani, Chaumet, and Bryant<sup>7</sup>; Draine and Goodman<sup>6</sup>; and Gutkowitz-Krusin and Draine<sup>9</sup> to allow for both finite wavelength and target geometry. We have tested the new polarizability prescription in calculations of absorption and scattering by spherical and ellipsoidal targets. These tests show that the SCLDR generally provides a significant increase in accuracy over previous prescriptions that took account of either finite wavelength or target geometry but not both. The finite wavelength corrections dominate in the  $|m - 1| \leq 0.5$  regime, whereas the geometric corrections are most important for  $\text{Im}(m) \geq 1$ ; including both allows the SCLDR prescription to perform

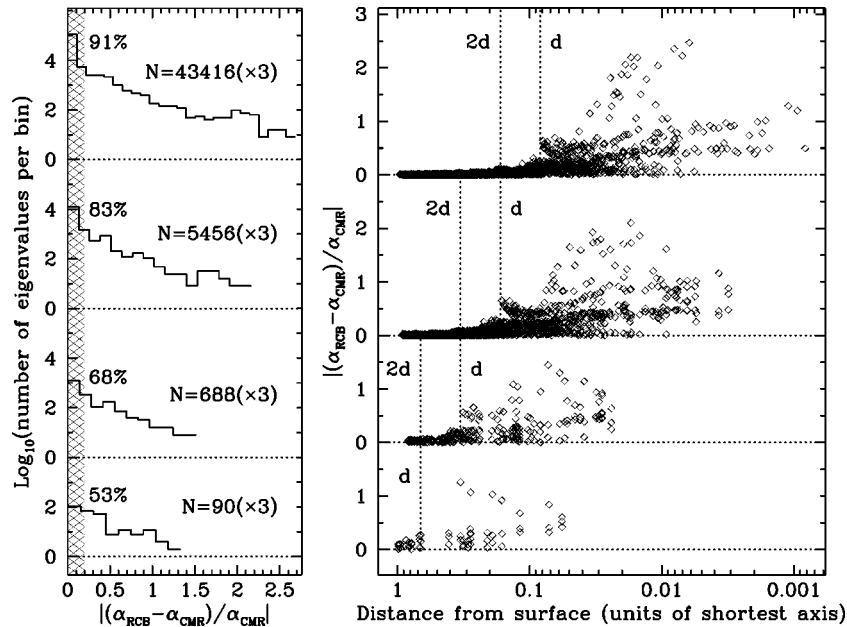


Fig. 7. Comparison of RCB and CMR polarizabilities. The left panel shows the distribution of polarizability eigenvalues for discrete dipole approximations to a 1:2:3 ellipsoid with  $m = 5 + 4i$  with  $N = 90, 688, 5456$ , and  $43,416$  dipoles. The shaded region corresponds to a fractional difference of 20% or less; the fraction of the eigenvalues within this region varies from 53% for  $N = 90$  ( $3d \times 6d \times 9d$  axes) to 91% for  $N = 43,416$  ( $24d \times 48d \times 72d$  axes). The right panel shows the fractional difference between RCB and CMR polarizabilities versus the distance (in units of the shortest axis) from the ideal ellipsoidal surface used to define the target (all dipole locations are interior to this surface). As expected, the RCB polarizability converges to the CMR polarizability for dipoles lying more than  $\sim 2d$  from the surface.

well throughout a large region in the complex  $m$  plane. The SCLDR technique is most easily applicable to targets for which there exists an analytical solution for the polarization in the presence of a static applied electric field, but it can be applied to any dielectric target (homogeneous or inhomogeneous, isotropic or anisotropic) provided that the electrostatic problem can at least be solved numerically to obtain the tensors  $\mathbf{C}_j$  [see Eq. (5)] at each dipole location.

## ACKNOWLEDGMENTS

This research was supported in part by National Science Foundation grants AST-9988126 and AST-0216105. M. J. Collinge also acknowledges support from a National Defense Science and Engineering graduate fellowship. The authors wish to thank Robert Lupton for making available the SM software package.

The authors can be contacted by e-mail at collinge@astro.princeton.edu or draine@astro.princeton.edu.

## REFERENCES

1. J. J. Goodman, B. T. Draine, and P. J. Flatau, "Application of fast-Fourier-transform techniques to the discrete dipole approximation," *Opt. Lett.* **16**, 1198–1200 (1990).
2. E. M. Purcell and C. R. Pennypacker, "Scattering and absorption of light by nonspherical dielectric grains," *Astrophys. J.* **186**, 705–714 (1973).
3. B. T. Draine, "The discrete-dipole approximation and its application to interstellar graphite grains," *Astrophys. J.* **333**, 848–872 (1988).
4. G. H. Goedecke and S. G. O'Brien, "Scattering by irregular inhomogeneous particles via the digitized Green's function algorithm," *Appl. Opt.* **27**, 2431–2438 (1988).
5. J. I. Hage and J. M. Greenberg, "A model for the optical properties of porous grains," *Astrophys. J.* **361**, 251–259 (1990).
6. B. T. Draine and J. Goodman, "Beyond Clausius–Mossotti: wave propagation on a polarizable point lattice and the discrete dipole approximation," *Astrophys. J.* **405**, 685–697 (1993).
7. A. Rahmani, P. C. Chaumet, and G. W. Bryant, "Coupled dipole method with an exact long-wavelength limit and improved accuracy at finite frequencies," *Opt. Lett.* **27**, 2118–2120 (2002).
8. C. F. Bohren and D. R. Huffman, *Absorption and Scattering of Light by Small Particles* (Wiley, New York, 1983).
9. D. Gutkiewicz-Krusin and B. T. Draine, "Propagation of electromagnetic waves on a rectangular lattice of polarizable points," <http://xxx.arxiv.org/abs/astro-ph/0403082>.
10. B. T. Draine and P. J. Flatau, "User guide for the discrete dipole approximation code DDSCAT (Version 5a10)," <http://xxx.arxiv.org/abs/astro-ph/0008151v3>, 1–42 (2000).
11. B. T. Draine and P. J. Flatau, "The discrete dipole approximation for scattering calculations," *J. Opt. Soc. Am. A* **11**, 1491–1499 (1994).